

## Density functional study of structure and bonding in lithium clusters Lin and their oxides LinO

R. O. Jones, A. I. Lichtenstein, and J. Hutter

Citation: *J. Chem. Phys.* **106**, 4566 (1997); doi: 10.1063/1.473498

View online: <http://dx.doi.org/10.1063/1.473498>

View Table of Contents: <http://jcp.aip.org/resource/1/JCPSA6/v106/i11>

Published by the AIP Publishing LLC.

---

### Additional information on J. Chem. Phys.

Journal Homepage: <http://jcp.aip.org/>

Journal Information: [http://jcp.aip.org/about/about\\_the\\_journal](http://jcp.aip.org/about/about_the_journal)

Top downloads: [http://jcp.aip.org/features/most\\_downloaded](http://jcp.aip.org/features/most_downloaded)

Information for Authors: <http://jcp.aip.org/authors>

## ADVERTISEMENT



**Goodfellow**  
metals • ceramics • polymers • composites  
70,000 products  
450 different materials  
small quantities *fast*

[www.goodfellowusa.com](http://www.goodfellowusa.com)

# Density functional study of structure and bonding in lithium clusters $\text{Li}_n$ and their oxides $\text{Li}_n\text{O}$

R. O. Jones and A. I. Lichtenstein

*Institut für Festkörperforschung, Forschungszentrum Jülich, D-52425 Jülich, Germany*

J. Hutter

*Max-Planck-Institut für Festkörperforschung, Heisenbergstr. 1, D-70569 Stuttgart, Germany*

(Received 9 September 1996; accepted 10 December 1996)

Density functional (DF) calculations have been performed for lithium clusters  $\text{Li}_n$  and their monoxides  $\text{Li}_n\text{O}$  with up to ten atoms. There are numerous stable structures, and new isomers have been found in each family. The structural patterns of the homonuclear and oxide clusters are quite distinct. The combination of DF calculations with molecular dynamics (MD) sheds light on the observed pseudorotation of  $\text{Li}_3$  and  $\text{Li}_5$ . We compare with available experimental data and discuss the bonding and structural patterns in the clusters and their oxides, which are often described as “hyperlithiated.” © 1997 American Institute of Physics. [S0021-9606(97)00511-4]

## I. INTRODUCTION

Lithium is the lightest element that is metallic under normal conditions and, together with its fellow alkali metals, has served for decades as a model “nearly free electron” system. It is only relatively recently, however, that the structural and bonding properties of small lithium clusters and of molecules containing lithium have received much attention. The results in both areas have been rather striking.

There is a single  $s$ -valence electron in the alkali elements, and it is not surprising that the energy surfaces of the clusters show shallower minima and less tendency to directional bonding than found in elements with  $p$ - and  $d$ -electrons (e.g., P and Fe, respectively). The structural flexibility and the absence of a clear guide to the most stable of the many possible structures present challenges to the theoretician and is well-known to experimentalists. The melting points of the alkali metals are low, ranging from 181 °C in Li down to 28.6 °C in Cs,<sup>1</sup> and there is clear evidence for pseudorotation in the electron spin resonance (ESR) and two-photon ionization spectra for  $\text{Li}_3$  (Refs. 2,3) and in ESR spectra for  $\text{Li}_5$ .<sup>4</sup> Thermochemical (mass-spectrometric) measurements have been made on clusters up to  $\text{Li}_5$  and provide estimates of the dissociation energies.<sup>5</sup> Lithium clusters with up to  $\sim 40$  atoms have been ionized and detected as cations, and their ionization potentials determined up to  $n=26$ .<sup>6</sup> Other spectroscopic data on  $\text{Li}_n$  clusters include optical absorption spectra of  $\text{Li}_4$ – $\text{Li}_8$ , measured using depletion spectroscopy,<sup>7</sup> and photoelectron spectroscopy on  $\text{Li}_4^-$ .<sup>8</sup> Measurements on the unimolecular dissociation of  $\text{Li}_n^+$  clusters<sup>9</sup> have provided information on the cohesive energies and dissociation paths of clusters with  $n=4$ – $42$ .

Extensive studies of neutral and charged Li clusters using Hartree–Fock (HF) based methods<sup>10</sup> have indicated that planar structures are preferred to  $n=6$ , with larger clusters (to  $\text{Li}_9$ ) comprising deformed tetrahedra. In conjunction with optical absorption data,<sup>7</sup> these calculations have been used to study the structures of the most stable isomers of  $\text{Li}_4$  to  $\text{Li}_8$ . The extension of the Hartree–Fock calculations to incorporate molecular dynamics (MD) (Ref. 11) has indicated

the existence of additional minima in the energy surface.

Small binary molecules containing lithium and other elements have received much attention in recent years, with lithiated molecules containing O, C, or Si showing unusual structures that appear to violate the octet rule, i.e., they have more than eight valence electrons occupying bonding orbitals. The first “hyperlithiated” molecule ( $\text{Li}_3\text{O}$ ) was identified experimentally,<sup>12</sup> and theory has led subsequently to unexpected structures in, for example,  $\text{CLi}_6$  ( $O_h$ ),<sup>13</sup>  $\text{Li}_4\text{O}$  ( $T_d$ ),<sup>14</sup>  $\text{Li}_4\text{Si}$  ( $C_{2v}$ ),<sup>15</sup>  $\text{Li}_5\text{O}^+$  ( $C_{3v}$ ),<sup>16</sup> and  $\text{Li}_{12}\text{C}$  ( $C_{4v}$ ).<sup>17</sup> There is little doubt that many unusual structures remain to be found.

We describe here the results of density functional (DF) calculations on the energy surfaces of lithium clusters  $\text{Li}_n$  and their monoxides  $\text{Li}_n\text{O}$  with up to ten atoms ( $\text{Li}_{10}$ ,  $\text{Li}_9\text{O}$ ). We have adopted a range of starting structures in all cases and have used both all-electron and pseudopotential calculations. The all-electron calculations use a Gaussian basis set,<sup>18</sup> and all geometries and vibration frequencies given below were determined using this method. In systems where pseudorotation is known to occur or where the nature of the most stable isomer is uncertain, we have used a combination of DF calculations with molecular dynamics (MD) (Ref. 19) at temperatures between 100–500 K to generate additional geometries and to shed light on structural changes. The MD/DF calculations use periodic boundary conditions (PBC) with a (simple cubic) unit cell with lattice constant 20 a.u., and a plane wave basis set with a single point ( $k=0$ ) in the Brillouin zone and an energy cutoff of 15 a.u. The electron-ion interaction is described by the non-local pseudopotential of Troullier and Martins,<sup>20</sup> using the  $d$ -component of the potential as the reference local part (“ $sp$ -nonlocality”).

All molecules were studied with both a local spin density (LSD) (Ref. 21) and a non-local modification (NLSD) involving the gradient of the density.<sup>22</sup> The MD/DF calculations were all performed with the LSD approximation. Unless otherwise stated, the spin degeneracies of the states calculated were the lowest possible. In some cases, such as Li–Li–O, a higher multiplicity is necessary (in this case a

TABLE I. Structure parameters for isomers of  $\text{Li}_n$  clusters,  $n=3-9$ , with energies  $\Delta E$  relative to the ground state (eV). Bond lengths  $d_{ij}$  in Å and bond angles  $\alpha_{ijk}$  in degrees. Other labels are defined in the figures.

Molecule	Symmetry	$\Delta E$
$\text{Li}_3$ 1(a)	$C_{2v}$	0.00
$d_{12}=2.82$ ; $d_{13}=3.37$ ; $\alpha_{123}=73.5$		
$\text{Li}_3$ 1(b)	$D_{\infty h}$	1.30
$d_{12}=2.89$		
$\text{Li}_4$ 1(c)	$D_{2h}$	0.00
$d_{12}=3.04$ ; $d_{24}=2.62$ ; $\alpha_{214}=51.0$		
$\text{Li}_4$ 1(d)	$C_{3v}$	0.31
$d_{12,23,13}=2.77$ ; $d_{14,24,34}=3.12$		
$\text{Li}_5$ 1(e)	$C_{2v}$	0.00
$d_{13,23}=2.63$ ; $d_{12}=3.00$ ; $d_{14,24}=3.09$ ; $d_{34}=2.96$		
$\text{Li}_5$ 1(f)	$C_{2v}$	0.23
$d_{12}=2.88$ ; $d_{15}=3.02$ ; $d_{45}=3.18$ ; $d_{25}=2.78$		
$\text{Li}_6$ 3(a)	$D_{4h}$	0.00
$d_{15}=2.82$ ; $d_{56}=2.49$		
$\text{Li}_6$ 3(b)	$C_{2v}$	0.45
$d_{12}=2.70$ ; $d_{23}=3.18$		
$\text{Li}_6$ 3(c)	$D_{3h}$	0.74
$d_{12}=2.89$ ; $d_{23}=2.95$		
$\text{Li}_7$ 3(d)	$C_{3v}$	0.00
$d_{15}=3.31$ ; $d_{17}=3.17$ ; $d_{12}=2.54$ ; $d_{27}=2.57$		
$\text{Li}_7$ 3(e)	$D_{5h}$	0.10
$d_{12}=2.91$ ; $d_{23}=3.05$ ; $d_{17}=2.61$		
$\text{Li}_8$ 3(f)	$D_{5h}$	0.00
$d_{18}=2.43$ ; $d_{12}=2.55$ ; $d_{23}=3.00$		

triplet). In others a small gap between the highest occupied and lowest unoccupied molecular orbitals (HOMO-LUMO gap) was taken as an indication that a state of higher multiplicity could have a similar energy. In Secs. II and III we present our results for clusters and oxides, respectively, including the changes in the binding energies with increasing cluster size. A discussion of trends and our concluding remarks follow in Sec. IV.

## II. RESULTS: LITHIUM CLUSTERS

In this section, we present the results obtained for structures and relative energies of isomers of neutral lithium clusters  $\text{Li}_n$  to  $n=10$ . Energies with respect to the most stable isomer are denoted  $\Delta E$ , and structural parameters for most are given in Table I. To simplify the figures, we have not labeled the atoms if the structure is derived from that of a smaller cluster. “Bonds” between Li atoms are shown if the atoms are separated by less than 3.1 Å. Atomic coordinates of all structures are available from the authors.<sup>23</sup>

### A. $\text{Li}_2$ , $\text{Li}_3$ , $\text{Li}_4$

The dimer  $\text{Li}_2$  is the lithium cluster for which the most detailed experimental information is available, and the calculated bond lengths and vibration frequencies of the  $^1\Sigma_g^+$  ground state (LSD: 2.80 Å, 325  $\text{cm}^{-1}$ ; NLSD: 2.80 Å, 322  $\text{cm}^{-1}$ ) are in reasonable agreement with the measured values (2.673 Å, 351.4  $\text{cm}^{-1}$ ).<sup>24</sup>

As in the other alkali trimers, the equilateral triangle ( $D_{3h}$ ) is not a stable doublet structure in  $\text{Li}_3$ , but undergoes a Jahn-Teller distortion to  $C_{2v}$  symmetry. There are three

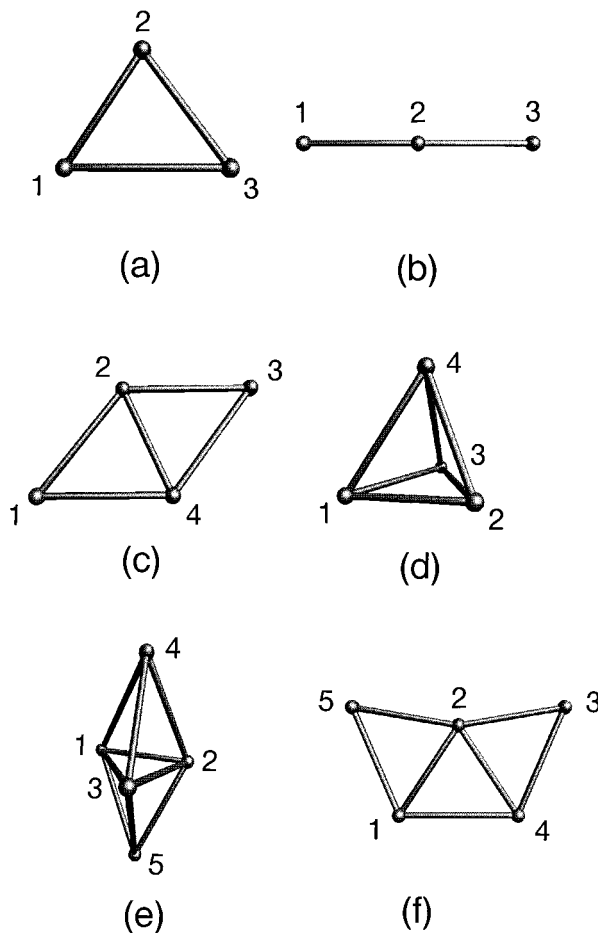


FIG. 1. Structures of  $\text{Li}_3$  [(a)  $C_{2v}$ , (b)  $D_{\infty h}$ ];  $\text{Li}_4$  [(c)  $D_{2h}$ , (d)  $C_{3v}$ ], and  $\text{Li}_5$  [(e,f), both  $C_{2v}$ ].

equivalent energy wells, and electron spin resonance (ESR) spectra of  $\text{Li}_3$  trapped in argon matrices<sup>2</sup> show that the molecule is fluxional, i.e., it undergoes a pseudorotation between the different minima. Two-photon ionization spectra of  $\text{Li}_3$  support this assignment,<sup>3</sup> showing three  $C_{2v}$  structures (bond length  $d=2.73$  Å, bond angle  $\alpha=72^\circ$ ) separated by a pseudorotation barrier of only 26  $\text{cm}^{-1}$  with a stationary point at (3.05 Å,  $50^\circ$ ).

The present calculations of the energy surfaces of  $\text{Li}_3$  lead to a similar picture. The energy difference between the most stable structure [Fig. 1(a)] (LSD:  $d_{12}=2.82$  Å,  $\alpha_2=73.5^\circ$ ; NLSD: 2.84 Å,  $73.2^\circ$ ) and the saddle point (LSD: 3.09 Å,  $52.1^\circ$ ; NLSD: 3.15 Å,  $51.6^\circ$ ) is minute (LSD: 110  $\text{cm}^{-1}$ ; NLSD: 165  $\text{cm}^{-1}$ ) and less than the calculated zero point vibrational energy (320  $\text{cm}^{-1}$ ). We have also performed combined MD/DF calculations on the lithium trimer. The geometry changes between two neighboring minima are very small and pseudorotation is evident in simulations at 20 K and 30 K.

We have investigated two higher-lying structures of  $\text{Li}_3$ : the quartet  $D_{3h}$  form ( $d_{12}=3.20$  Å,  $\Delta E=1.31$  eV) is not Jahn-Teller distorted, and the linear form [1(b),  $d_{12}=2.89$  Å] lies a further 0.09 eV higher in the LSD calculations. The NLSD approximation results in very similar energy differ-

ences and a small increase in the bond lengths. This is a general feature of our results, and we give NLSD structures below only if they differ appreciably from these trends. Cohesive energies calculated using the two approximations are significantly different and will be discussed in Secs. II G ( $\text{Li}_n$  clusters) and III F ( $\text{Li}_n\text{O}$  molecules).

HF-based calculations<sup>10</sup> predict that the most stable isomer of  $\text{Li}_4$  is the rhombus [singlet,  $D_{2h}$ , 1(c)], and this is also found here. A flattened, Jahn-Teller distorted tetrahedron [triplet,  $C_{2v}$ , 1(d)] lies 0.31 eV higher. The structural parameters are given in Table I.

## B. $\text{Li}_5$

HF-based calculations<sup>10</sup> predict the lithium pentamer to be planar ( $C_{2v}$ ), with a three-dimensional  $C_{2v}$  structure the next most stable. Pseudopotential DF calculations,<sup>25</sup> on the other hand, favor the three-dimensional structure by 0.22 eV, and this result is supported by the present calculations. We find two local minima with  $C_{2v}$  symmetry [1(e,f)], with the pyramidal form more stable by 0.23 eV (NLSD: 0.16 eV), and the energy surface shows several other minima and stationary points with  $\Delta E < 0.4$  eV. The unstable structures include a rectangular pyramid ( $C_{2v}$ ,  $\Delta E = 0.21$  eV), which has two imaginary frequencies and distorts to structure 1(e), and a planar  $D_{2h}$  structure that lies between two equivalent planar  $C_{2v}$  forms and less than 0.1 eV above them. The quartet state corresponding to 1(e) is a (stable)  $D_{3h}$  bipyramid with  $\Delta E = 0.26$  eV.

The situation is reminiscent of earlier results on aluminum clusters,<sup>26</sup> where planar structures were favored up to  $\text{Al}_4$ , and planar and three-dimensional isomers had very similar energies in the pentamer.  $\text{Al}_n$  clusters also show a near degeneracy for different spin states for  $n = 5-6$ . A near-degeneracy between quartet tetrahedral and doublet rhombic structures of was found in recent calculations on the  $\text{Li}_4^-$  anion.<sup>27</sup>

ESR measurements have been performed on Li clusters deposited at 77 K in an adamantane matrix and annealed to temperatures above 200 K.<sup>4</sup> The spectra show that the  $\text{Li}_n$  clusters present have  $n$  magnetically equivalent nuclei (i.e., are fluxional), and the coupling constants show that  $n > 3$ . While  $\text{Li}_5$  is an obvious candidate, the authors do not think that they detected a pseudorotating planar isomer of this isomer, and they do not exclude  $\text{Li}_7$ . The pseudopotential DF calculations mentioned above,<sup>25</sup> however, showed that the isotropic spin population for the planar ( $C_{2v}$ ) structure agrees better with the measured value. These authors then proposed a pseudorotation mechanism based on geometry changes within a plane.

Insight into possible mechanisms of structural change in  $\text{Li}_5$  is provided by MD/DF simulations. A section of a typical run at 100 K is shown in Fig. 2 and illustrates two interesting points: (a) If the energy surface is relatively flat, as in this case, the simulation need not pass through the minima of the energy surface (here the planar and tbp structures), even at 100 K. (b) Nevertheless, it shows that the interchange of the planar and three-dimensional structures is relatively easy un-

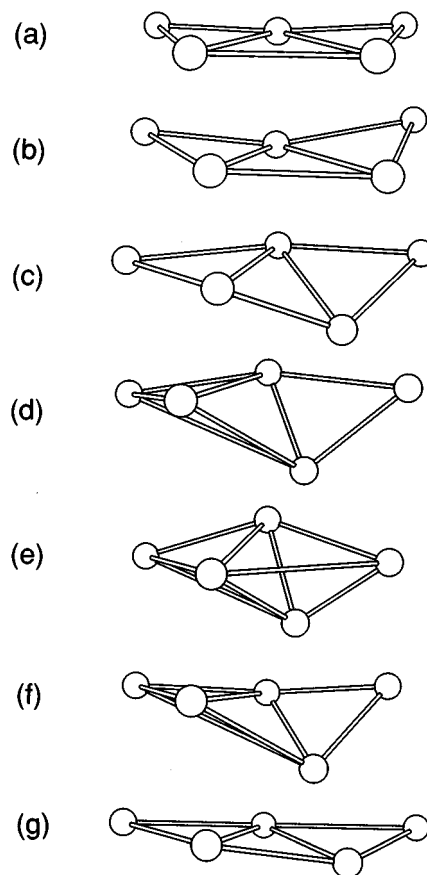


FIG. 2. Pseudorotation in  $\text{Li}_5$ . MD/DF simulation performed at 100 K.

der the conditions of this simulation, and suggests a simple mechanism — the twisting of the central triangle — for pseudorotation between equivalent trigonal bipyramids (tbp) via an almost planar form. An alternative transition state for this process would be a square pyramid (sp,  $C_{4v}$ ), as proposed by Berry<sup>28</sup> for structural changes in  $\text{PF}_5$ . In the lithium pentamer, we can understand this process by stretching one of the base diagonals of the (unstable) square pyramid.  $\Delta E$  for this structure is less than 0.4 eV, and we have seen above that the value for the related  $C_{2v}$  rectangular prism is only 0.26 eV. Since a planar  $D_{2h}$  structure is also a transition state between and 0.10 eV above equivalent planar  $C_{2v}$  forms, as mentioned above, there are then several possible mechanisms for isomerization in  $\text{Li}_5$ . We discuss Berry pseudorotation further in the context of  $\text{Li}_5\text{O}$  in Sec. III C.

## C. $\text{Li}_6$

HF-based calculations<sup>10</sup> show that three structures have similar energies: a planar  $D_{3h}$  structure, a quasiplanar pentagonal pyramid ( $C_{5v}$ ) with one atom slightly above the plane, and a (non-planar) tripyramid ( $C_{2v}$ ). The most stable structure ( $D_{3h}$ ) was the only one of the three to give an optical absorption spectrum consistent with the measured data.<sup>7</sup>

Both LSD and NLSD calculations give several isomers with comparable energies and favor three-dimensional over

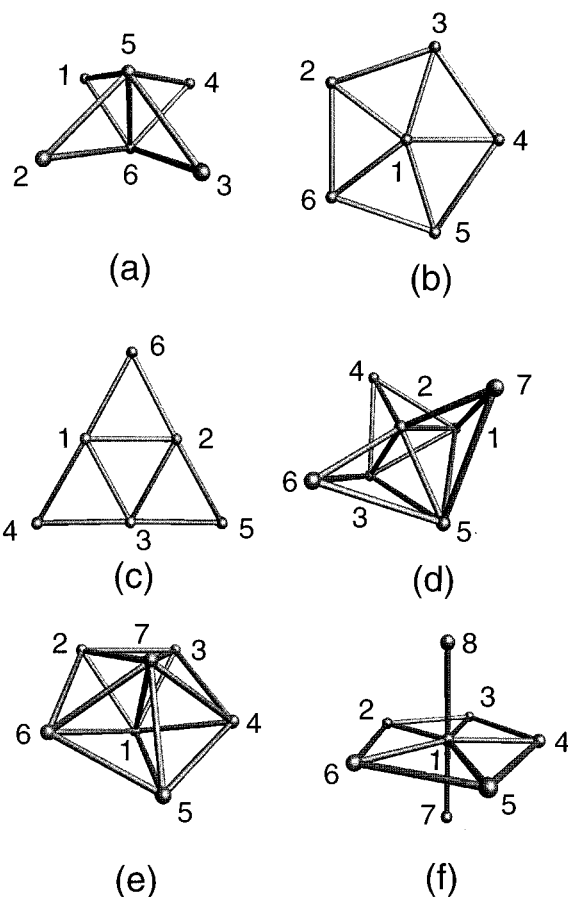


FIG. 3. Structures of  $\text{Li}_6$  [(a)  $D_{4h}$ , (b)  $D_{5h}$ , (c)  $D_{3h}$ ];  $\text{Li}_7$  [(d)  $C_{3v}$ , (e)  $D_{5h}$ ], and  $\text{Li}_8$  [(f)  $D_{5h}$ ].

planar structures, but there are significant differences from the HF structures. The  $C_{2v}$  tripyramid found in the latter distorts here to the more symmetric flattened octahedron [ $D_{4h}$ , 3(a)] that is the most stable form we have found. The planar pentagonal structure [ $D_{5h}$ , 3(b) — this may be viewed as a more symmetric form of the  $C_{5v}$  pentagonal pyramid] is 0.45 eV higher, followed by the planar  $D_{3h}$  structure [3(c), this comprises four approximately equilateral triangles and is the most stable in the HF calculations] an additional 0.29 eV higher. The symmetries  $D_{3h}$ ,  $D_{4h}$ , and  $D_{5h}$  all have twofold representations. In the present cases the highest occupied orbitals are doubly degenerate and fully occupied, so that a Jahn-Teller distortion does not occur. A Jahn-Teller distortion would occur in the corresponding positive ion,  $\text{Li}_6^+$ .

#### D. $\text{Li}_7$

The earlier HF-based calculations<sup>10</sup> indicate a most stable isomer of pentagonal bipyramidal form [ $D_{5h}$ , Fig. 3(e)], followed by a  $C_{3v}$  isomer [3(d)] formed by capping three of the faces of a tetrahedron. Similar structures are found in the present work, although the order is reversed [the  $D_{5h}$  structure is more stable by 0.10 eV].

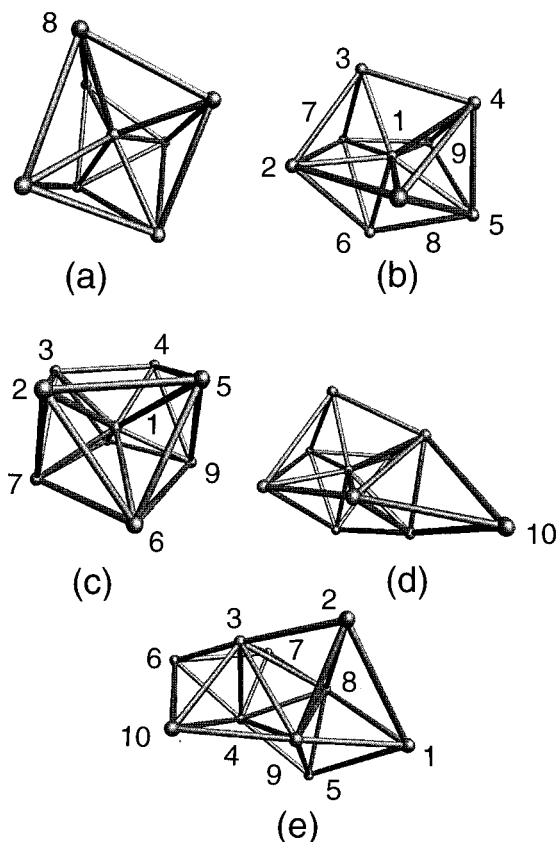


FIG. 4. Structures of  $\text{Li}_8$  [(a)  $T_d$ ],  $\text{Li}_9$  (b,c), and  $\text{Li}_{10}$  (d,e).

ESR spectra have been reported for  $\text{Li}_7$  clusters formed by codepositing Li with excess Ar in a helium cryostat.<sup>29</sup> The situation is different from that in  $\text{Li}_3$  and  $\text{Li}_5$ , in that the unpaired electron has a distinctive symmetry that is consistent with a pentagonal bipyramidal ( $D_{5h}$ ) structure.

#### E. $\text{Li}_8$

Two isomers of  $\text{Li}_8$  were considered in the HF-based work,<sup>7,10</sup> a tetrahedron with all four faces capped ( $T_d$ ) and a related  $D_{2d}$  structure. The dominant features of the calculated optical absorption spectrum were found to be similar,<sup>7</sup> and it was concluded that either or both structures could contribute to the measured spectrum.

The most stable structure found in the present calculations is, however, a further member in the  $D_{5h}$  sequence  $\text{Li}_6$  [3(b)]  $\rightarrow$   $\text{Li}_7$  [3(e)]  $\rightarrow$   $\text{Li}_8$  [3(f)]. Structure Fig. 4(a) ( $T_d$ ,  $\Delta E = 0.52$  eV) is just as obviously related to the most stable form of  $\text{Li}_7$  [3(d)]. The atoms of the central tetrahedron are separated from each other by 2.80 Å, and from the outer atoms by 2.93 Å. The second most stable isomer ( $C_{2v}$ ,  $\Delta E = 0.24$  eV) comprises a rhombus (sides 2.99 Å, bond angle 63.7°) atop a rectangle (sides 2.88 Å, 2.99 Å). It is related to isomer 4(b) of  $\text{Li}_9$  (see below) and is reminiscent of the crown shape of the sulfur octamer. Other stationary points in the energy surface were either considerably higher

in energy (examples being the related triplet states) or had imaginary frequencies and were unstable.

### F. $\text{Li}_9$ - $\text{Li}_{10}$

The number of isomers increases dramatically with increasing cluster size, so that the identification of the most stable becomes rapidly more difficult. For  $\text{Li}_9$  and  $\text{Li}_{10}$  we have studied structures derived by adding atoms to stable isomers of smaller clusters, removing them from larger ones, structures proposed by other authors, and those found by scaling the stable structures of clusters of other elements. We have also used MD/DF simulations to cover larger regions of configuration space and to guide our choice of starting structures for the all-electron calculations. The most stable structures found for  $\text{Li}_9$  and  $\text{Li}_{10}$  are shown in Fig. 4, but we expect that there are additional isomers with comparable energies.

A stable  $C_s$  isomer of  $\text{Li}_9$  [4(b)] is related to the  $\text{Li}_8$  isomers Figs. 3(d) and 4(a) by adding outer atoms, while structure 4(c) has higher symmetry ( $C_{4v}$ ) and can be viewed as the rhombus/rectangle form of  $\text{Li}_8$  with an added central atom. These  $\text{Li}_9$  structures and their energies are remarkably similar, with  $\Delta E$  values for 4(c) of 0.06 eV (LSD) and less than 0.01 eV (NLSD). They are not related by a Jahn-Teller distortion, however, as the uppermost occupied orbital in the  $C_{4v}$  structure is singly degenerate. Given the approximations inherent in these calculations, it would be unwise to make a definite prediction of the most stable isomer.

The most stable form that we found for  $\text{Li}_{10}$  [ $C_1$ , 4(d)] is obtained by capping the 4(b) isomer of  $\text{Li}_9$ . A second isomer [ $C_{2v}$ , 4(d),  $\Delta E=0.25$  eV] may be viewed as two interlocking pentagonal rings. The existence of regular and distorted pentagons is a recurring feature of the structures we have found in the Li clusters.

### G. Cohesive energies

The cohesive energy is defined as the energy required to separate the most stable form of a cluster into its constituent atoms, and is usually expressed as an energy per atom. It has been estimated for lithium clusters in two ways: from high-temperature gas phase mass spectroscopy<sup>5</sup> and from combining the measured dissociation energies of the  $\text{Li}_n^+$  clusters<sup>9</sup> with the ionization potentials.<sup>6</sup> Both sets of results are shown in Fig. 5, where they are compared with the present calculated values (LSD, NLSD) and the values extrapolated from MRD-CI calculations for geometries scaled from the HF values.<sup>10</sup> We note that the measured cohesive energy of bulk Li ( $n \rightarrow \infty$ ) is 1.66 eV.<sup>1</sup>

The overall agreement between theory and experiment is satisfactory, and we note that the use of the NLSD approximation leads to cohesive energies that are lower than the LSD values. This is a common effect in clusters of elements that form  $sp$ -bonds, an example being  $\text{P}_n$  and  $\text{As}_n$  clusters, where the LSD approximation leads to overestimates in the cohesive energy of  $\sim 1$  eV.<sup>30</sup> These findings are consistent with the observation<sup>31</sup> that LSD estimates of exchange energy differences will be less reliable if there is a change in

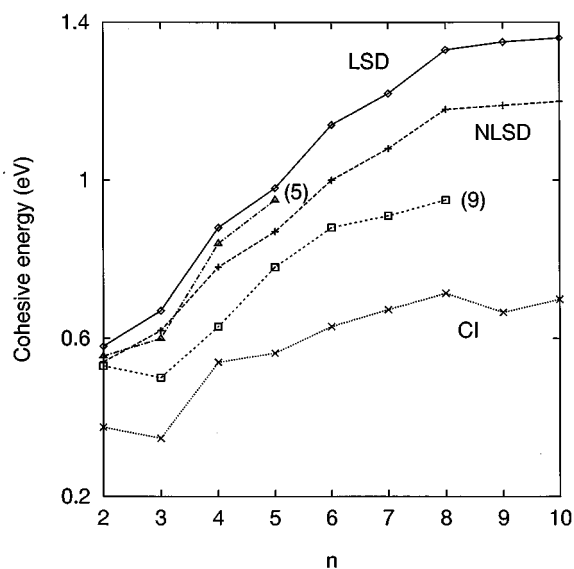


FIG. 5. Calculated (LSD, NLSD) and measured [Refs. 5 and 9] cohesive energies (binding energies per atom) for  $\text{Li}_n$  clusters to  $n=10$ . Also shown are values obtained by extrapolating MRD-CI calculations for scaled HF geometries [Ref. 10].

the angular nodal structure of the orbitals. The non-local modifications were shown to move charge away from the nuclei, leading to weaker and longer bonds, and to an increasing difference between LSD and NLSD cohesive energies with increasing cluster size.

Although  $p$ -orbitals play a role in bonding between Li atoms, the (nodeless)  $s$ -character dominates. The LSD estimates of the binding energy are much closer to experiment than in the group 15 clusters, and the effects of gradient corrections are smaller. We see in Fig. 5 that the different experimental techniques give rise to somewhat different results, and it is difficult to say whether the LSD or NLSD estimates are better. Although the NLSD approximation often improves the estimates of energy differences, this is not necessarily the case. The rare gas dimers, for example, have well depths that are overestimated by LSD calculations, but there is no minimum in the energy curves at all if gradient corrections are included.<sup>32</sup>

### III. RESULTS: LITHIUM CLUSTER OXIDES

In this section, we present the results for the structures of isomers of neutral lithium cluster oxides  $\text{Li}_n\text{O}$  to  $n=9$ , and discuss bonding trends. In all figures we label atom 1 (black) as oxygen, the remaining (grey) atoms are Li. Li-O "bonds" are shown if the atoms are separated by less than 2.3 Å. The single oxygen atom has a dramatic effect on the structures of small lithium clusters, which may not be surprising, since oxygen has six valence electrons and lithium only one. A comparable effect is also evident in the solid state, where the density of lithium atoms in the oxide  $\text{Li}_2\text{O}$  is over 80% higher than that in crystalline lithium itself,<sup>33</sup> and there is a very similar effect in sodium.<sup>34</sup>

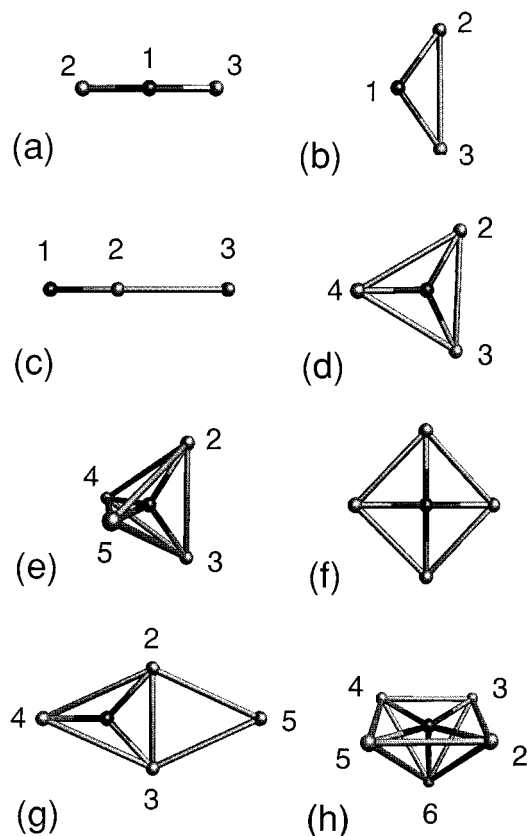


FIG. 6. Structures of  $\text{Li}_2\text{O}$  (a-c);  $\text{Li}_3\text{O}$  (d);  $\text{Li}_4\text{O}$  (e-g);  $\text{Li}_5\text{O}$  (h).

### A. $\text{LiO}$ , $\text{Li}_2\text{O}$ , $\text{Li}_3\text{O}$

Small lithium monoxide clusters were investigated almost 20 years ago by HF calculations ( $\text{LiO}$ ,  $\text{LiOLi}$ ,  $\text{LiLiO}$ )<sup>35</sup> and thermochemical measurements ( $\text{LiO}$ ,  $\text{Li}_2\text{O}$ ,  $\text{Li}_3\text{O}$ ).<sup>12,36</sup> More recent studies will be cited below. Stoichiometric clusters of the form  $(\text{Li}_2\text{O})_n$  have also been studied recently using MD/DF methods.<sup>37</sup>

HF calculations<sup>35</sup> gave a bond length in  $\text{LiO}$  of 1.71 Å and a vibration frequency of 829  $\text{cm}^{-1}$ , and the present results [LSD: 1.72 Å, 784  $\text{cm}^{-1}$ ; NLSD: 1.74 Å, 760  $\text{cm}^{-1}$ ] follow a common trend for DF calculations to give bonds that are longer than HF values. Compared with the measured dissociation energy (3.49 eV),<sup>24</sup> the present results (LSD: 4.36 eV, NLSD: 3.89 eV) also show the familiar picture of a substantial LSD overestimate being improved by non-local modifications.

HF calculations on the  $\text{LiOLi}$  molecule<sup>35</sup> gave a linear singlet ground state [ $D_{\infty h}$ ,  $^1\Sigma_g^+$  Fig. 6(a)] with bond length 1.62 Å and vibration frequencies 145 ( $\pi_u$ ), 839 ( $\sigma_g$ ), and 1091 ( $\sigma_u$ )  $\text{cm}^{-1}$ . The MD/DF calculations of Finocchi and Noguera<sup>37</sup> gave the same bond length, and the  $\sigma_g$ - and  $\sigma_u$ -vibration frequencies were found to be 810 and 1075  $\text{cm}^{-1}$ , respectively. The bond lengths found in the present calculations are slightly longer (LSD: 1.64 Å, NLSD: 1.65 Å), but the vibration frequencies (144, 819, 1081  $\text{cm}^{-1}$ ) are close to the earlier estimates. A bent triplet state [ $C_{2v}$ , 6(b)] with  $d_{12}=1.80$  Å and  $\alpha_{213}=107.4^\circ$  lies 2.57 eV higher.

The ground state of the  $\text{LiLiO}$  molecule is a linear triplet state [ $^3\Pi$ , 6(c)], characterized by a very long Li-Li bond (HF: 3.29 Å,<sup>35</sup> LSD: 2.87 Å) and a Li-O bond similar to that in the diatomic molecule (HF, LSD: 1.73 Å).<sup>35</sup> This is the simplest example in the present work of a “hypervalent” molecule, where the number of bonds on the central Li atoms appears to be greater than the number of electrons.

We have noted above that  $\text{Li}_3\text{O}$  was the first “hyperlithiated” molecule to be prepared,<sup>12</sup> and it has been studied theoretically by several authors. HF calculations by Schleyer *et al.*<sup>14,38</sup> indicated that a planar  $C_{2v}$  structure [6(d)] was the most stable. Although more detailed calculations<sup>39</sup> favored a  $D_{3h}$  structure, the lower symmetry was found in recent second order Møller-Plesset (MP2) and complete active space (CAS) SCF calculations.<sup>40</sup> However, the energy surface is very flat, and the barrier against pseudorotation is less than 0.03 eV. The present calculations also give a  $C_{2v}$  structure (with three Li-O bonds close to 1.68 Å) that is weakly perturbed from the equilateral triangle ( $D_{3h}$ ).

### B. $\text{Li}_4\text{O}$

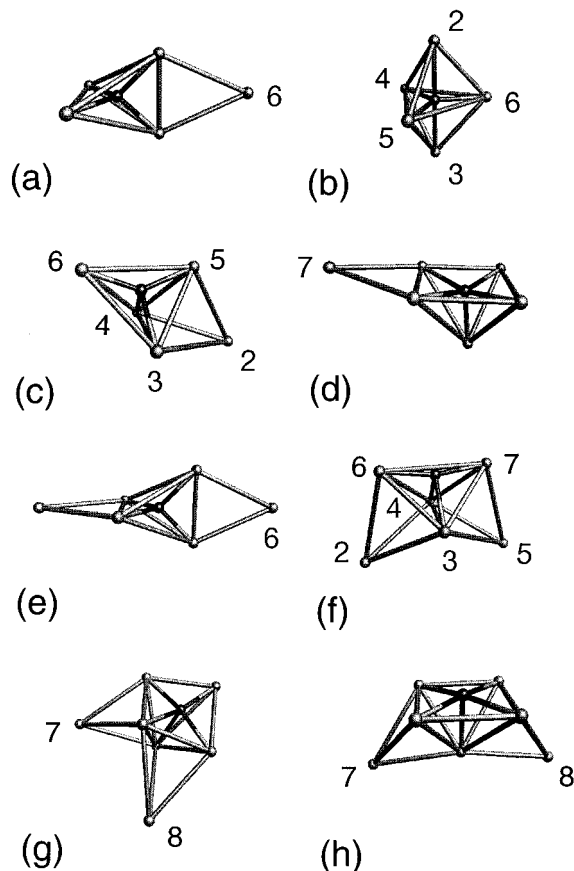
$\text{Li}_4\text{O}$  and  $\text{Li}_5\text{O}$  were studied theoretically by Schleyer and coworkers<sup>14,38</sup> and identified by Wu using high temperature mass spectrometry.<sup>41</sup> The most stable structure in the HF calculations was tetrahedral [ $T_d$ , 6(e)], with a Li-O bond of 1.728 Å. A second minimum of the energy surface was the  $C_{2v}$  form [6(g),  $\Delta E=0.79$  eV]. This has Li-O bonds with a normal length ( $d_{14}=1.623$  Å,  $d_{12}=1.689$  Å), while the Li-Li separation is very long indeed ( $d_{25}=3.234$  Å).

A similar picture results from the present calculations. The  $T_d$  (singlet) state gives the most stable structure, with  $d_{\text{LiO}}=1.74$  Å,  $d_{\text{LiLi}}=2.85$  Å. A related triplet state lies 0.57 eV higher. The  $C_{2v}$  structure [6(g),  $\Delta E=1.19$  eV] has the structural parameters  $d_{12}=1.69$  Å,  $d_{14}=1.62$  Å,  $d_{23}=2.44$  Å,  $d_{25}=3.04$  Å. The planar  $D_{4h}$  structure [6(f),  $\Delta E=0.83$  eV] occurs as a unit of larger clusters. It is a stationary point in the energy surface of  $\text{Li}_4\text{O}$ , but is unstable and distorts readily to the  $T_d$  form, with  $d_{\text{LiO}}=1.78$  Å,  $d_{\text{LiLi}}=2.51$  Å.

### C. $\text{Li}_5\text{O}$

The  $\text{Li}_5\text{O}$  molecule is particularly interesting, as it has several isomers with similar energies separated by low energy barriers. HF calculations<sup>38</sup> were performed for the  $C_{3v}$  bipyramid isomer of  $\text{Li}_5\text{O}$  [Fig. 7(b)], which is also a stable structure in the present work ( $d_{12}=1.82$  Å,  $d_{15}=1.87$  Å,  $d_{25}=2.61$  Å,  $d_{23}=3.16$  Å). Two others are slightly ( $<0.03$  eV) more stable. The rectangular pyramid [ $C_{2v}$ , 6(h), a Jahn-Teller distortion of a square pyramid,  $C_{4v}$ ] is the most stable in the LSD calculations ( $d_{12}=1.85$  Å,  $d_{16}=1.84$  Å,  $d_{23}=2.46$  Å,  $d_{34}=2.72$  Å), with energy slightly below that of a  $C_{2v}$  structure 7(a), which is related to isomer 6(e) of  $\text{Li}_4\text{O}$  by adding a Li atom with large (3.04 Å) separations from atoms 2 and 3. In the NLSD calculations the latter structure is slightly ( $\sim 0.07$  eV) more stable than 6(h) and 7(a), which are almost degenerate.

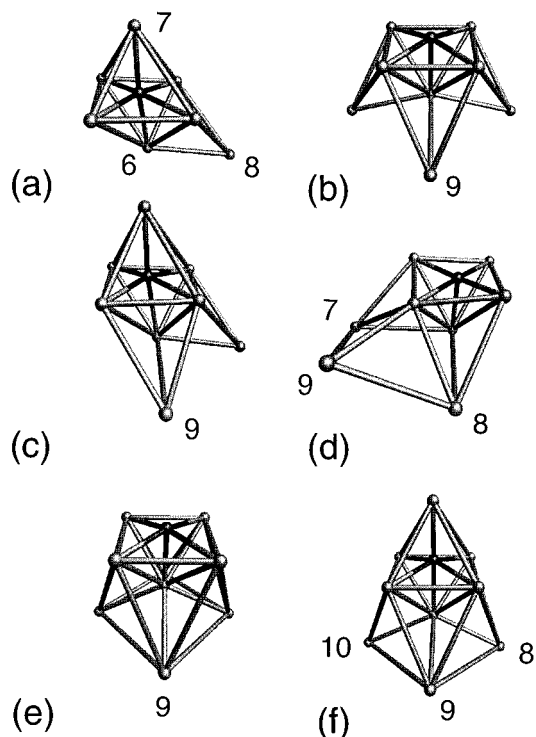


FIG. 7. Structures of  $\text{Li}_5\text{O}$  (a-c);  $\text{Li}_6\text{O}$  (d-f);  $\text{Li}_7\text{O}$  (g,h).

The most stable isomers of  $\text{Li}_5\text{O}$  show five-fold coordination of the central atom. A discussion of two such molecules ( $\text{PF}_5$  and  $\text{PCl}_5$ ) led Berry<sup>28</sup> to propose a pseudorotation mechanism trigonal bipyramid  $\rightarrow$  square pyramid  $\rightarrow$  trigonal bipyramid, in which the isomerization takes place by deformation of the bond angles at the central atom. The positive ion  $\text{Li}_5\text{O}^+$  has the same number of valence electrons (10) as  $\text{PF}_5$ , and HF-based calculations<sup>16</sup> show a very small barrier ( $\sim 1.2$  kcal/mole) to pseudorotation  $D_{3h} \rightarrow C_{4v} \rightarrow D_{3h}$ . These calculations also predicted the existence of a trigonal bipyramid ( $C_{3v}$ ) structure of  $\text{Li}_5\text{O}^+$  with lower coordination and containing a  $\text{Li}_4$  subcluster, and this was also found to be stable in the present calculations. The corresponding neutral structure [ $C_s$ , 7(c)] is an unstable stationary point in the energy surface only slightly ( $< 0.05$  eV) above the minima noted above. We see below that the pattern of an oxygen atom in a lithium “cage” attached to a Li subcluster is common in the larger clusters.

#### D. $\text{Li}_6\text{O}$

For neutral  $\text{Li}_6\text{O}$  (twelve valence electrons) the first (Hartree–Fock) calculations<sup>38</sup> found a minimum for a  $D_{3d}$  distortion of a regular octahedron ( $O_h$ ). Considerations of the Jahn–Teller effect of hexalithide structures<sup>42</sup> suggested that the most stable structure might have even lower symmetry, and HF and MP2 calculations<sup>43</sup> showed, in fact, a  $D_{2d}$

FIG. 8. Structures of  $\text{Li}_7\text{O}$  (a);  $\text{Li}_8\text{O}$  (b-d);  $\text{Li}_9\text{O}$  (e,f).

isomer with two bidentate  $\text{Li}_3$  groups [7(e)]. This structure bears an obvious relationship to isomer 7(b) of  $\text{Li}_5\text{O}$ . The most stable isomer in the present LSD calculations is, however, 7(d), which bears an equally obvious relationship to another isomer of  $\text{Li}_5\text{O}$  [6(h)]. This is followed by Figs. 7(e) and 7(f) ( $C_{2v}$ ), both of which have  $\Delta E = 0.07$  eV. The latter is related by capping to the unstable form 7(c) of  $\text{Li}_5\text{O}$ .

It is interesting to study the structures related to the regular octahedron. A quintet state with this structure is stable ( $d_{\text{LiO}} = 1.90$  Å), but lies 0.50 eV above 7(d). A  $D_{3d}$  structure with  $d_{\text{LiO}} = 1.92$  Å and bond angles  $\alpha_{\text{LiOLi}}$  distorted from  $90^\circ$  by  $\sim 4^\circ$  is 0.20 eV above the most stable (LSD) isomer.

A similar picture results from the NLSD calculations, but isomer 7(e) is about 0.04 eV more stable than 7(d), with 7(f) an additional 0.05 eV higher. The energy differences between these structures and those derived from the octahedron are close to the LSD values. The small energy differences between Figs. 7(a,b,c) in both sets of calculations indicates that all three are candidates for the most stable isomer.

#### E. $\text{Li}_7\text{O}$ , $\text{Li}_8\text{O}$ , $\text{Li}_9\text{O}$

We have found three stable isomers of  $\text{Li}_7\text{O}$  with structures that are related to the most stable form of  $\text{Li}_5\text{O}$  [6(h)], and the most stable in both LSD and NLSD calculations is 7(g) ( $C_s$ ). In the LSD calculations 7(h) ( $C_{2v}$ ) and Fig. 8(a) (a distorted  $C_{3v}$  structure) are 0.14 eV and 0.20 eV higher, respectively, and the NLSD relative energies are very similar.



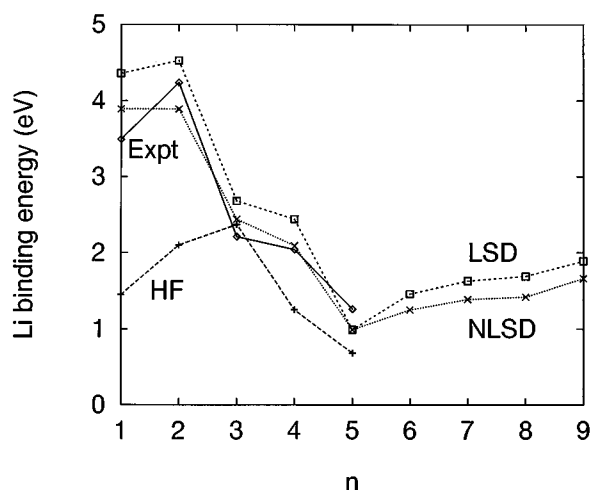


FIG. 9. Energy differences  $\text{Li}_n\text{O} \rightarrow \text{Li}_{n-1}\text{O} + \text{Li}$ . Experiment [Refs 12,41]; Hartree-Fock (HF) [Refs. 14,38]; LSD, NLSD [this work].

Three structures found for  $\text{Li}_8\text{O}$  [8(b,c,d)] have  $C_s$  symmetry and are derived by capping the  $\text{Li}_7\text{O}$  structures. The most stable is 8(b), which is 0.25 eV more stable than the others in the LSD calculations. The energy spread is less in the NLSD calculations, but Figs. 8(c,d) are 0.06 eV and 0.19 eV, respectively, less stable than 8(b). The two most stable structures found in  $\text{Li}_9\text{O}$  are shown in Figs. 8(a,b). The former ( $C_{4v}$ ) is  $\sim 0.1$  eV more stable in both LSD and NLSD calculations.

## F. Bonding trends

The structures of  $\text{Li}_n\text{O}$  isomers are often found by adding a Li atom to the neighboring smaller cluster, with a small change in the atomic positions of the latter. This is particularly evident for  $n \geq 5$ , and is reflected in the binding energies of the binding energies of the added Li atom, which are shown in Fig. 9 for the most stable isomers. The trend for  $n > 5$  is very similar to that found for the cohesive energies of  $\text{Li}_n$  [Fig. 5]. There is a steady increase in the binding energy as  $n$  increases, and the LSD estimates of this energy are  $\sim 0.2$  eV higher than the NLSD values.

The even-odd alternation in the binding energies of Li atoms in  $\text{Li}_n$  clusters (Fig. 5) and in  $\text{Li}_n\text{O}$  (Fig. 9) reflect the relative stability of both oxide and cluster for even values of  $n$ , where all orbitals are doubly occupied. However, there are pronounced differences between the two plots for  $n = 2 - 5$ . While the cohesive energy of  $\text{Li}_n$  increases steadily from the dimer value towards the bulk cohesive energy (1.66 eV, Ref. 1), the binding energy of Li to the oxide clusters increases initially — the Li-O-Li molecule satisfies the octet rule — and then drops rapidly to a minimum at  $\text{Li}_5\text{O}$ . This difference is also seen in the thermochemical estimates of the Li binding energy.

Oxide clusters larger than  $\text{Li}_2\text{O}$  appear to have more “bonds” than available electron pairs, and have been referred to as “hyperlithiated.” The role of oxygen in determining the structure is crucial, as it has six valence electrons

to one in Li. For  $n = 3, 4$ , the lithium atoms form shells around the O atom in two- and three-dimensions, respectively, and for  $\text{Li}_5\text{O}$ , where the binding energy is a minimum, there are several structures with almost the same energy and small barriers between them. Still larger clusters arise increasing the size of the Li subcluster attached to the  $\text{Li}_5\text{O}$  units, and the binding energy increases as noted above.

## IV. DISCUSSION AND CONCLUDING REMARKS

We have performed an extensive series of density functional (DF) calculations on lithium clusters and their monoxides with up to ten atoms ( $\text{Li}_{10}$  and  $\text{Li}_9\text{O}$ , respectively). A variety of starting structures has been used in each, and we have generated many more by combining DF calculations with molecular dynamics. Previously unknown structures have been found in both families, but there are many possible isomers in systems of this size, and there is little doubt that other structures exist that are energetically favorable.

Lithium shares with the other alkali metals and hydrogen the simplest valence electron configuration, a single  $s$ -electron. Although  $sp$ -hybridization is stronger in Li than in the other alkalis,<sup>44</sup> Li clusters show a weaker tendency to directional bonding than elements with  $sp$ - and  $sd$ -valence configurations. The energy minima are less pronounced and the barriers between them lower. MD/DF simulations show that both  $\text{Li}_3$  and  $\text{Li}_5$  are fluxional, consistent with the pseudorotation observed in these molecules.

Much of the earlier work on the structures of  $\text{Li}_n$  clusters has used HF-based methods. We have found a number of new structures, and we have shown that the structures of larger clusters can often be found by adding atoms to the stable structures of smaller ones. While the largest clusters that we have studied ( $\text{Li}_{10}$ ) show few signs of patterns found in the bcc crystalline form, we note that interatomic distances close to the nearest neighbor separation in bulk Li (bcc, 3.03 Å) occur in smaller clusters. Examples are the sides of the rhombus in  $\text{Li}_4$  [1(c), 3.04 Å], the sides joining the apices to the base of  $\text{Li}_5$  [1(f), 3.02 Å], and the pentagonal edges in the  $D_{5h}$  isomers of  $\text{Li}_7$  [3(e), 3.05 Å] and  $\text{Li}_8$  [3(f), 3.00 Å]. The calculated cohesive energies [Fig. 5] show results that are consistent with earlier experience with other elements: overestimates with the LSD approximation to the exchange-correlation energy, improved values with the gradient corrected (NLSD) modification.

The study of the structures of  $\text{Li}_n\text{O}$  clusters has been fascinating. We have noted in Sec. II that the density of lithium atoms in bulk  $\text{Li}_2\text{O}$  is much higher than in bulk Li,<sup>33</sup> and the effect of an oxygen atom on the cluster structures is no less dramatic. The oxide clusters  $\text{Li}_n\text{O}$  are generally more compact than their  $\text{Li}_n$  counterparts, and there are many novel structures with more than eight valence electrons. Insight into such molecules has been provided by the groups of Schleyer, Marsden, and others. In a study of  $\text{Li}_n\text{O}$  molecules up to  $n = 6$ , for example, Schleyer<sup>38</sup> showed that the charge (Mulliken) on the oxygen atom increased little beyond that in Li-O-Li, with the additional electrons contributing primarily to Li-Li bonding. Calculations of high-spin states in Li clusters with up to six atoms also showed the existence of bound molecules without spin-paired valence electrons.<sup>45</sup> This pic-

ture is consistent with the present work, where we find that the binding energy of the added Li atom falls from  $\text{Li}_2\text{O}$  to  $\text{Li}_5\text{O}$  and then increases with a pattern similar to that found in  $\text{Li}_n$  clusters.

If the initial structure of one of the larger clusters (e.g.,  $\text{Li}_7\text{O}$ ,  $\text{Li}_8\text{O}$ ) is taken to have the O atom in a central position, this atom moves towards the "surface" as the structure optimization proceeds, leaving behind a Li subcluster [e.g., Figs. 7(g) and 8(d)]. This is such a dramatic process that it is natural to speculate that it could occur in much larger clusters or at a surface. Unfortunately, the highly exothermic reaction of O with Li means that the oxidation of the surface is very difficult to study.

We emphasize again the variety of structures that arises in both  $\text{Li}_n$  and  $\text{Li}_n\text{O}$  families. In  $\text{Li}_5\text{O}$ , in particular, there are several structures with almost the same energy, separated by small energy barriers. The calculated structures also show interesting patterns involving  $\text{Li}_4\text{O}$  (tetrahedral),  $\text{Li}_5\text{O}$  [square ( $C_{4v}$ ) or rectangular ( $C_{2v}$ ) pyramids], and  $\text{Li}_6\text{O}$  [approximately octahedral] units. The tetrahedron is the most stable form of  $\text{Li}_4\text{O}$ , and the capped tetrahedra in  $\text{Li}_5\text{O}$  [Fig. 7(a)] and  $\text{Li}_6\text{O}$  [Fig. 7(e)] are only slightly higher in energy than the pyramidal structures Figs. 6(h) and 7(d), respectively. Four-fold coordination of the O atom is not favored in larger clusters, where the present calculations prefer five-fold over six-fold coordination of the O atom, although the energy differences are often small.

Many of the structures found in the present work are predictions, and it would be interesting to have both more experimental information about the structures of both  $\text{Li}_n$  and  $\text{Li}_n\text{O}$  systems, as well as calculations using other methods. A reliable description of the interaction between Li and O atoms is a prerequisite for performing calculations on lithium glasses such as  $\beta$ -eucryptite,  $\text{LiAlSiO}_4$ . The DF calculations that we are currently carrying out should provide useful insight into these systems.

## ACKNOWLEDGMENTS

This work was supported by the MaTech Program of the Bundesminister für Bildung, Wissenschaft, Forschung und Technologie, Bonn. R.O.J. thanks C. H. Wu for suggesting the study of molecules containing lithium, and I. Bytheway for helpful discussions and comments on an earlier version of the manuscript.

<sup>1</sup>K. A. Gschneidner, Jr., *Solid State Phys.* **16**, 275 (1964).

<sup>2</sup>D. A. Garland and D. M. Lindsay, *J. Chem. Phys.* **78**, 2813 (1983).

<sup>3</sup>P. Dugourd, J. Chevalere, M. Broyer, J. P. Wolf, and L. Wöste, *Chem. Phys. Lett.* **175**, 555 (1990).

<sup>4</sup>J. A. Howard, H. A. Joly, R. Jones, P. P. Edwards, R. J. Singer, and D. E. Logan, *Chem. Phys. Lett.* **204**, 128 (1993).

<sup>5</sup>C.H. Wu, *J. Chem. Phys.* **65**, 3181 (1976) [ $\text{Li}_2$ ,  $\text{Li}_3$ ]; *J. Phys. Chem.* **87**, 1534 (1983) [ $\text{Li}_4$ ]; *J. Chem. Phys.* **91**, 546 (1989) [ $\text{Li}_5$ ].

<sup>6</sup>P. Dugourd, D. Rayane, P. Labastie, B. Vezin, J. Chevalere, and M. Broyer, *Chem. Phys. Lett.* **197**, 433 (1992).

<sup>7</sup>J. Blanc, V. Bonačić-Koutecký, M. Broyer, J. Chevalere, P. Dugard, J. Koutecký, C. Scheuch, J. P. Wolf, and L. Wöste, *J. Chem. Phys.* **96**, 1793 (1992).

<sup>8</sup>H. W. Sarkas, S. T. Arnold, J. H. Hendricks, and K. H. Bowen, *J. Chem. Phys.* **102**, 2653 (1995).

<sup>9</sup>C. Bréchnignac, H. Busch, P. Cahuzac, and J. Leygnier, *J. Chem. Phys.* **101**, 6992 (1994).

<sup>10</sup>I. Boustani, W. Pewestorf, P. Fantucci, V. Bonačić-Koutecký, and J. Koutecký, *Phys. Rev. B* **35**, 9437 (1987) [ $\text{Li}_n^-$ ,  $\text{Li}_n^+$ ]; I. Boustani and J. Koutecký, *J. Chem. Phys.* **88**, 5657 (1988) [ $\text{Li}_n^-$ ].

<sup>11</sup>P. Fantucci, V. Bonačić-Koutecký, J. Jellinek, M. Wiechert, R. J. Harrison, and M. F. Guest, *Chem. Phys. Lett.* **250**, 47 (1996).

<sup>12</sup>H. Kudo, C.H. Wu, and H. R. Ihle, *J. Nucl. Mater.* **78**, 380 (1978); C. H. Wu, H. Kudo, and H. R. Ihle, *J. Chem. Phys.* **70**, 1815 (1979).

<sup>13</sup>P. v.R. Schleyer, E.-U. Würthwein, E. Kaufmann, T. Clark, and J. A. Pople, *J. Am. Chem. Soc.* **105**, 5930 (1983).

<sup>14</sup>P. v.R. Schleyer, E.-U. Würthwein, and J. A. Pople, *J. Am. Chem. Soc.* **104**, 5839 (1982).

<sup>15</sup>P. v.R. Schleyer and A. E. Reed, *J. Am. Chem. Soc.* **110**, 4453 (1982).

<sup>16</sup>J. Ivanich, O. P. Charkin, and C. J. Marsden, *Russ. J. Inorg. Chem.* **40**, 955 (1995). This paper studies several pentalithide clusters  $\text{AlLi}_5$  with ten valence electrons.

<sup>17</sup>J. Ivanich and C. J. Marsden, *J. Chem. Soc. Chem. Commun.* **1989**, 1356.

<sup>18</sup>DGauss program from the UniChem package of Cray Research, Inc. The calculations used a triple zeta Gaussian orbital basis with polarization functions (TZ94+p) and the TZ94 auxiliary basis.

<sup>19</sup>CPMD version 3.0 written by J. Hutter, Max-Planck-Institut für Festkörperforschung, Stuttgart, 1996.

<sup>20</sup>N. Troullier and J. L. Martins, *Phys. Rev. B* **43**, 1993 (1991).

<sup>21</sup>We use the parameterization of the exchange-correlation energy of the homogeneous electron gas given by S. H. Vosko, L. Wilk, and M. Nusair, *Can. J. Phys.* **58**, 1200 (1980).

<sup>22</sup>The gradient-corrected functional used the modification to the exchange energy of A. D. Becke, *Phys. Rev. A* **38**, 3098 (1988) and the modified correlation energy functional of J. P. Perdew, *Phys. Rev. B* **33**, 8822 (1986).

<sup>23</sup>Contact R. O. Jones (internet: r.jones@kfa-juelich.de).

<sup>24</sup>K. P. Huber and G. Herzberg, *Molecular Spectra and Molecular Structure. IV. Constants of Diatomic Molecules* (Van Nostrand Reinhold, New York, 1979).

<sup>25</sup>R. Kawai, J. F. Tombrello, and J. H. Weare, *Phys. Rev. A* **49**, 4236 (1994).

<sup>26</sup>R. O. Jones, *J. Chem. Phys.* **99**, 1194 (1993).

<sup>27</sup>B. K. Rao, P. Jena, and A. K. Ray, *Phys. Rev. Lett.* **76**, 2878 (1996).

<sup>28</sup>R. S. Berry, *J. Chem. Phys.* **32**, 933 (1960). This process is referred to as "Berry pseudorotation." For a discussion and further references, see I. Ugi, J. Dugundij, R. Kopp, and D. Marquarding, *Perspectives in Theoretical Chemistry* (Springer, Berlin Heidelberg, 1984).

<sup>29</sup>D. A. Garland and D. M. Lindsay, *J. Chem. Phys.* **80**, 4761 (1984).

<sup>30</sup>P. Ballone and R. O. Jones, *J. Chem. Phys.* **100**, 4941 (1994).

<sup>31</sup>R. O. Jones and O. Gunnarsson, *Rev. Mod. Phys.* **61**, 689 (1989).

<sup>32</sup>J. M. Pérez-Jordá and A. D. Becke, *Chem. Phys. Lett.* **233**, 134 (1995).

<sup>33</sup>The density of solid Li is  $0.534 \text{ g cm}^{-3}$ , that of  $\text{Li}_2\text{O}$   $2.103 \text{ g cm}^{-3}$  [*Gmelins Handbuch der anorganischen Chemie. Lithium*, 8. Auflage, edited by E. H. E. Pietsch (Verlag Chemie, Weinheim, 1960), p. 166 and p. 260]. The density of Li atoms in  $\text{Li}_2\text{O}$  is then  $\sim 0.98 \text{ g cm}^{-3}$ . The lattice constant of bcc Li is  $3.502 \text{ Å}$  (*ibid.*, p. 164), so that the nearest neighbor separation is  $3.03 \text{ Å}$ .

<sup>34</sup>The density of solid Na at  $20^\circ\text{C}$  is  $0.966 \text{ g cm}^{-3}$ , that of  $\text{Na}_2\text{O}$   $2.39 \text{ g cm}^{-3}$  [*Gmelins Handbuch der anorganischen Chemie. Natrium*, 8. Auflage, Ergänzungsband 2, edited by E. H. E. Pietsch (Verlag Chemie, Weinheim, 1965), pp. 521 and 812].

<sup>35</sup>D. T. Grow and R. M. Pitzer, *J. Chem. Phys.* **67**, 4019 (1977).

<sup>36</sup>H. Kimura, M. Asano, and K. Kubo, *J. Nucl. Mater.* **92**, 221 (1980).

<sup>37</sup>F. Finocchi and C. Noguera, *Phys. Rev. B* **53**, 4989 (1996).

<sup>38</sup>P. v.R. Schleyer, in *New Horizons in Quantum Chemistry*, edited by P. O. Löwdin and B. Pullman (Reidel, Dordrecht, 1983), p. 95.

<sup>39</sup>E. I. Würthwein, P. v.R. Schleyer, and J. A. Pople, *J. Am. Chem. Soc.* **106**, 6973 (1984).

<sup>40</sup>M. Gutowski and J. Simons, *J. Phys. Chem.* **98**, 8326 (1994).

<sup>41</sup>C. H. Wu, *Chem. Phys. Lett.* **139**, 357 (1987).

<sup>42</sup>A. M. Mebel', N. M. Klimenko, and O. P. Charkin, *Russ. J. Inorg. Chem.* **36**, 245 (1991).

<sup>43</sup>J. Ivanich, C. J. Marsden, and D. M. Hassett, *J. Chem. Soc. Chem. Commun.* **1993**, 822 (1993).

<sup>44</sup>J. Harris and R. O. Jones, *Phys. Rev. A* **19**, 1813 (1979).

<sup>45</sup>M. N. Glukhovtsev and P. v.R. Schleyer, *Isr. J. Chem.* **33**, 455 (1993).